Stratospheric Vacillation Cycles[1]

JAMES R. HOLTON AND CLIFFORD MASS

Department of Atmospheric Sciences, University of Washington, Seattle 98195

(Manuscript received 30 April 1976, in revised form 23 July 1976)

ABSTRACT

A quasi-geostrophic β-plane channel model is used to study wave-mean flow interaction in the stratosphere. The zonal mean circulation in the model is driven by differential radiative heating (parameterized in terms of a "Newtonian cooling") and by horizontal eddy heat fluxes due to vertically propagating planetary waves excited by steady forcing at the lower boundary. We find that for sufficiently low-amplitude wave forcing the response is a steady stratospheric circulation very close to radiative equilibrium conditions. However, when the wave forcing is raised beyond a critical amplitude (typically of order 150 m) the response is no longer steady; rather, the mean zonal flow and eddy components oscillate quasi-periodically. We conclude that oscillations in stratospheric long waves do not necessarily reflect oscillating tropospheric forcing but may occur even in the presence of steady forcing.

1. Introduction

The winter seasonal mean circulation of the Northern Hemisphere stratosphere consists primarily of planetary waves of zonal wavenumbers 1 and 2 superposed on a zonal westerly vortex. The planetary waves are quasi-stationary in phase but tend to fluctuate in amplitude. Occasionally the anomalous amplification of such waves leads to an enormous enhancement of the poleward eddy heat flux which in turn leads to a reversal of the normal pole-to-equator temperature gradient over a sufficient depth of the stratosphere so that the mean polar westerlies are replaced by easterlies. This sequence of events, known as a major stratospheric warming, has been the subject of many observational and theoretical studies [see Quiroz *et al.* (1975) for a review]. However, relatively little attention has been given to the weaker wave-mean flow oscillations which occur at about 1 to 4 week intervals throughout the winter.

These quasi-periodic oscillations, sometimes called "minor warmings," have been discussed recently by Madden (1975) who analyzed eight winter seasons of 30 mb Northern Hemisphere data. Madden's analysis revealed 1–3 week oscillations in the zonal mean temperature gradient at high latitudes which were coherent with oscillations in the eddy heat flux across 60°N. Madden further showed that the oscillating eddy heat fluxes can, to a large extent, be accounted for by the presence of traveling wave modes which alternately constructively and destructively interfere with the quasi-stationary waves.

[1] Contribution No. 382, Department of Atmospheric Sciences, University of Washington.

Unlike the major sudden stratospheric warmings, minor warmings are not confined to the Northern Hemisphere. Observations of such oscillations in the Southern Hemisphere, based on satellite infrared radiance data, have been reported by Harwood (1975) and Leovy and Webster (1976). Leovy and Webster also included an interesting comparison between the stratospheric oscillations in the zonal mean, wavenumber 1 and wavenumber 2 thickness fields for the winter season of 1972–1973 in each hemisphere.

It is generally agreed that most planetary waves in the stratosphere are produced and maintained by vertical propagation of wave energy from the troposphere. For stationary wave modes a number of dynamical models have confirmed the primacy of tropospheric forcing [see Holton (1975) for a review of the literature]. In addition, various mechanistic models (Matsuno, 1971; Geisler, 1974; Holton, 1976) have demonstrated that the essential features of major sudden warmings can be simulated by computing the time-dependent stratospheric response to an anomalous enhancement in the tropospheric forcing of planetary wavenumbers 1 or 2. Minor warming cycles which resemble the quasi-periodic oscillations observed by Madden (1975) have been reproduced in some stratospheric simulation models (e.g., Trenberth, 1971). However, a satisfactory mechanistic understanding of the origin of such oscillations has not yet been developed. There is evidence that some stratospheric wave oscillations may merely represent a direct response to oscillations in the amplitude of the tropospheric wave sources (Muench, 1965; Hirota and Sato, 1969; Deland, 1973; Leovy and Webster, 1976). However, not all oscillations in stratospheric long

waves can be traced back to oscillations in tropospheric forcing.

The purpose of this paper is to demonstrate, by use of a simple mechanistic model, that wave-mean flow oscillations in the stratosphere may exist even when the tropospheric forcing is completely steady. In fact we will show that for our model a critical amplitude of the tropospheric forcing exists which separates two radically different stratospheric regimes: a steady regime for forcing less than the critical amplitude, and an oscillating regime for forcing greater than the critical amplitude. In the latter regime the oscillations are associated with a baroclinic energy conversion cycle analogous to the amplitude vacillation cycle observed in laboratory annulus experiments [for a recent reference see Pfeffer *et al.* (1974)]. For this reason we will refer to these oscillations as *stratospheric vacillation cycles*.

2. The dynamical model

Geisler (1974) has shown that the essential dynamics of sudden stratospheric warmings can be simulated, at least qualitatively, with a quasi-geostrophic β-plane channel model. Our model is similar to Geisler's except that our mean zonal wind has a sine jet meridional variation, while Geisler specified a mean flow distribution independent of latitude. Use of the sine jet profile enables us to develop a wave-mean flow interaction model in which the meridional dependence is separated in a less *ad hoc* fashion than in Geisler's model. But more importantly, Simmons (1974) has shown that, for a basic-state wind with constant westerly vertical shear, the vertical penetration of forced planetary waves is much greater when the mean wind has a sine jet profile which roughly models the observed polar night jet, rather than a latitudinally independent distribution.

Development of quasi-geostrophic models for the study of wave-mean flow interaction has been reviewed by Holton (1975). In such models the wave fields are assumed to be governed by the linearized quasi-geostrophic potential vorticity equation which in log pressure coordinates is

$$\left(\frac{\partial}{\partial t}+\bar{u}\frac{\partial}{\partial x}\right)q'+\beta_e\frac{\partial\psi'}{\partial x}+\frac{f_0^2}{\rho_s}\frac{\partial}{\partial z}\left(\frac{\alpha\rho_s}{N^2}\frac{\partial\psi'}{\partial z}\right)=0, \quad (1)$$

where

$$q'\equiv\nabla^2\psi'+\frac{1}{\rho_s}\frac{\partial}{\partial z}\left(\frac{f_0^2}{N^2}\rho_s\frac{\partial\psi'}{\partial z}\right)$$

is the perturbation potential vorticity and

$$\beta_e\equiv\beta-\frac{\partial^2\bar{u}}{\partial y^2}-\frac{1}{\rho_s}\frac{\partial}{\partial z}\left(\rho_s\frac{f_0^2}{N^2}\frac{\partial\bar{u}}{\partial z}\right)$$

is the gradient of the basic state potential vorticity. Here ψ' is a geostrophic streamfunction; f_0 is the Coriolis parameter at 60°N latitude; $N^2[=4\times10^{-4}\ \mathrm{s}^{-2}]$ is the buoyancy frequency squared; β is the meridional derivative of the Coriolis parameter at 60°N; $\rho_s[\equiv\rho_0\times\exp(-z/H)]$ is a standard density, where ρ_0 is the density at $z=10$ km and $H[=7\ \mathrm{km}]$ is a mean scale height; $\alpha[=\alpha(z)]$ is a Newtonian cooling rate coefficient; and all other symbols are as defined in Holton (1975).

Again in the notation of Holton (1975) equations for the zonal mean flow are

$$\frac{\partial\bar{u}}{\partial t}-f_0\bar{v}=0, \quad (2)$$

$$f_0\bar{u}=-\frac{\partial\bar{\Phi}}{\partial y}, \quad (3)$$

$$\frac{\partial}{\partial t}\left(\frac{\partial\bar{\Phi}}{\partial z}\right)+N^2\bar{w}=-\alpha\left(\frac{\partial\bar{\Phi}}{\partial z}-\frac{R\bar{T}^*}{H}\right)-\frac{\partial}{\partial y}\overline{(v'\Phi_z')}, \quad (4)$$

$$\frac{\partial\bar{v}}{\partial y}+\frac{1}{\rho_s}\frac{\partial}{\partial z}(\rho_s\bar{w})=0, \quad (5)$$

where $\bar{T}^*\equiv\bar{T}^*(y,z)$ is a "radiative equilibrium" temperature field. Following Dickinson (1969) we combine (2)–(5) to form a prediction equation for $\bar{u}$:

$$\frac{\partial}{\partial t}\left[\frac{\partial^2\bar{u}}{\partial y^2}+\frac{f_0^2}{N^2}\frac{1}{\rho_s}\frac{\partial}{\partial z}\left(\rho_s\frac{\partial\bar{u}}{\partial z}\right)\right]=-\frac{f_0^2}{N^2}\frac{1}{\rho_s}\frac{\partial}{\partial z}\left[\alpha\rho_s\left(\frac{\partial\bar{u}}{\partial z}-\frac{\partial u_R}{\partial z}\right)\right]+\frac{\partial^2}{\partial y^2}\left[\frac{f_0^2}{N^2}\frac{1}{\rho_s}\frac{\partial}{\partial z}(\rho_s\overline{v'\psi_z'})\right], \quad (6)$$

where u_R is a mean zonal wind field which is set equal to the actual mean wind $\bar{u}$ at the lower boundary and satisfies thermal wind balance with the radiative equilibrium temperature field, i.e.,

$$f_0\frac{\partial u_R}{\partial z}=-\frac{R}{H}\frac{\partial\bar{T}^*}{\partial y}.$$

Thus in this model the mean zonal flow is driven by two separate physical processes: a parameterized diabatic heating which relaxes the thermal wind field toward a radiative equilibrium state (which in the results shown here is assumed independent of time), and eddy potential vorticity transport by the planetary waves.

We now specialize (1)–(6) by assuming that the flow is confined to a β-plane channel centered at 60°N with a meridional extent L equal to 60° latitude. The channel is bounded below by the tropopause

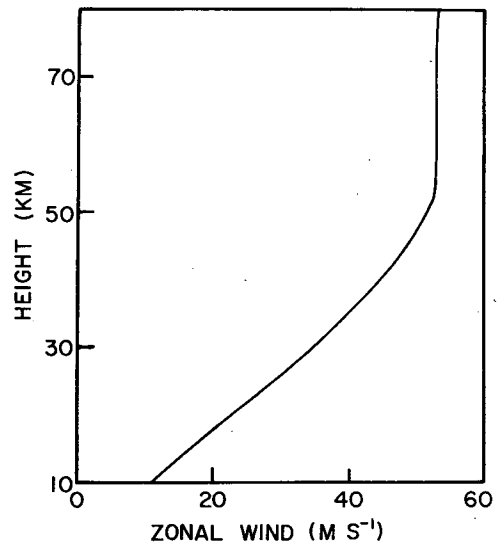

FIG. 1. Initial mean zonal wind profile at mid-channel.

($z_B \approx 10$ km) and above by the mesopause ($z_T \approx 80$ km). The condition of zero normal flow across the lateral boundaries requires that $\psi'=0$ and $\bar{v}=0$ at $y=0, L$. If we assume that $\bar{u}=0$ initially at $y=0, L$, we see from (2) that $\bar{u}=0$ for all time at $y=0, L$. At the lower boundary we specify both the mean flow and wave perturbation by setting

$$\bar{u}=\bar{u}_B(y), \quad \psi'=\psi_B(y,t), \quad \text{at } z=z_B.$$

At the upper boundary we assume that the energy density of the wave perturbation vanishes and that the zonal mean thermal wind vanishes,[2] i.e.,

$$\rho_s^{\frac{1}{2}}\psi'=0, \quad \frac{\partial \bar{u}}{\partial z}=0, \quad \text{at} \quad z=z_T.$$

Following Simmons (1974) we assume that the wave perturbation consists of a single zonal harmonic component and that the meridional dependence of both the ψ' and $\bar{u}$ fields can be represented by the lowest terms in a Fourier sine series expansion

$$\psi'=\mathrm{Re}[\Psi(z,t)\exp(ikx)]\exp(z/2H)\sin ly + (\text{higher order terms}), \quad (7a)$$

$$\bar{u}=U_0(z,t)\sin ly+(\text{higher order terms}). \quad (7b)$$

Here $l=3/a$ and $k=s/(a\cos\pi/3)$ where a is the earth's radius and $s=1, 2\cdots$ is the zonal planetary wavenumber.

We next substitute the assumed solutions [(7)] for ψ' and $\bar{u}$ into (1) and (6). When this is done all terms which are quadratic in $\bar{u}$ and ψ' [e.g., $\bar{u}\partial q'/\partial x$ in (1)] will have y dependencies of the form $\sin^2 ly$. Therefore, in order to separate the y dependence we expand $\sin^2 ly$ in a Fourier sine series[3]

$$\sin^2 ly=\epsilon \sin ly+(\text{higher order terms}), \quad (8)$$

where $\epsilon \equiv 8/(3\pi)$ and the higher order terms contribute less than 5% of the total variance. We thus find that $\Psi(z,t)$ and $U_0(z,t)$ must satisfy the following pair of prognostic equations:

$$\left(\frac{\partial}{\partial t}+ik\epsilon U_0\right)\left[-(k^2+l^2)+\frac{f_0^2}{N^2}\left(\frac{\partial^2}{\partial z^2}-\frac{1}{4H^2}\right)\right]\Psi + \beta_e' ik\Psi+\frac{f_0^2}{N^2}\left(\frac{\partial}{\partial z}-\frac{1}{2H}\right)\left[\alpha\left(\frac{\partial}{\partial z}+\frac{1}{2H}\right)\Psi\right]=0, \quad (9)$$

$$\frac{\partial}{\partial t}\left[-l^2U_0+\frac{f_0^2}{N^2}\left(\frac{\partial^2 U_0}{\partial z^2}-\frac{1}{H}\frac{\partial U_0}{\partial z}\right)\right] = -\frac{f_0^2}{N^2}e^{z/H}\frac{\partial}{\partial z}\left[\alpha e^{-z/H}\left(\frac{\partial U_0}{\partial z}-\frac{\partial U_R}{\partial z}\right)\right] + \frac{l^2k\epsilon}{2}\frac{f_0^2}{N^2}e^{z/H}\,\mathrm{Im}\left[\Psi\frac{\partial^2\Psi^*}{\partial z^2}\right]. \quad (10)$$

Here

$$\beta_e' \equiv \beta+\epsilon l^2 U_0-\frac{f_0^2}{N^2}\epsilon\left(\frac{\partial^2 U_0}{\partial z^2}-\frac{1}{H}\frac{\partial U_0}{\partial z}\right),$$

$$U_R(z,t)=u_R(\sin ly)^{-1},$$

and Ψ^* is the complex conjugate of Ψ and Im is the imaginary part. Eqs. (9) and (10) together with appropriate initial conditions and the upper and lower boundary conditions given above constitute a well-posed initial value problem for the evolution of the fields of ψ' and $\bar{u}$. We have solved this set numerically using an implicit time differencing scheme with a time step of $\Delta t=1$ h and a vertical grid distance of $\Delta z=2.5$ km. (For a more detailed discussion of the differencing scheme see the Appendix.)

3. Model parameters

In the experiments reported below we have computed the response of the model stratosphere to a switched-on wave forcing at the lower boundary. We assume that the flow is initially zonally symmetric and that $U_0(z)$ has a vertical distribution typical for observed winter mean conditions at 60°N (Fig. 1). We then impose a geopotential height perturbation at the lower boundary by letting

$$\Psi(z_B,t)=gh(t)/f_0, \quad (11)$$

where $h(t)=h_B[1-\exp(-t/\tau)]$. Here $\tau=2.5\times10^5$ s and h_B, the asymptotic steady-state amplitude of the

[2] For comparison we also tried $\bar{u}=0$ at $z=z_T$. There was no significant difference in the results except quite near $z=z_T$.

[3] Simmons (1974) expanded β in a sine series so that all terms in (1) had a sine square dependence to lowest order in the steady-state case. The present procedure is more suitable for the time dependent problem.

forcing, is a specified parameter. One of the chief purposes of this paper is to describe the dependence of the simulations on the parameter h_B.

Differential radiative heating is a major energy source for stratospheric motions. In our model we have parameterized radiative heating using a simple linear Newtonian cooling approximation in which the heating rate depends on two parameters: a Newtonian cooling coefficient α and a "radiative equilibrium" zonal wind shear $\partial U_R/\partial z$. For simplicity we have let $\partial U_R/\partial z = 3$ m s^{-1} km^{-1}, independent of height. This shear rate corresponds to a radiative equilibrium temperature difference of nearly 40 K between the northern and southern boundaries of the β-plane channel; a value which is in rough agreement with the detailed radiative equilibrium calculations of Leovy (1964) for winter solstice conditions. It is well-known that the rate coefficient for Newtonian cooling varies rather strongly with height (Dickinson, 1973). In order to model the rapid increase of α with height up to ~50 km, and to insure that waves are damped out before reaching the upper boundary at 80 km, we have let α vary according to the simple functional dependence

$$\alpha(z) = \{1.5 + \tanh[(z-35)/7]\} \times 10^{-6} \text{ s}^{-1}, \quad (12)$$

where z is given in km. At most levels between 20 and 50 km the values of α given by (12) are in approximate agreement with those used by Trenberth (1971) in his stratospheric general circulation model. The implied radiative damping times range from ~20 days near 20 km to ~4 days near 50 km.

4. Results and conclusions

As mentioned in the Introduction we have found that two entirely different solution regimes exist for this model depending on the amplitude of the lower boundary forcing. In Fig. 2 examples of the evolution of the zonal mean flow at 25 km are shown for both regimes in the case of planetary wavenumber 2 forcing. After an initial period of about 8 days the two cases evolve in dramatically different fashions. For boundary forcing $h_B = 140$ m the zonal flow asymptotically approaches a state near radiative equilibrium; for $h_B = 145$ m the zonal flow switches over to easterlies in a manner characteristic of sudden stratospheric warmings and then continues to oscillate from westerly to easterly with a period of about 65 days. The wavenumber 2 perturbation streamfunction (not shown) exhibits analogous behavior. In the $h_B = 140$ m case the waves undergo damped oscillations and eventually approach a steady-state standing wave pattern in which the eddy heat flux is nearly zero. In the $h_B = 145$ m case, on the other hand, the waves continually oscillate in a quasi-regular fashion, amplifying and decaying as the transient components alternately constructively and destructively interfere with the stationary components. The result is a strongly oscillating eddy heat flux (and hence potential vorticity flux) which drives the oscillations in the mean zonal flow, which in turn give rise to the continued excitation of transient wave components.

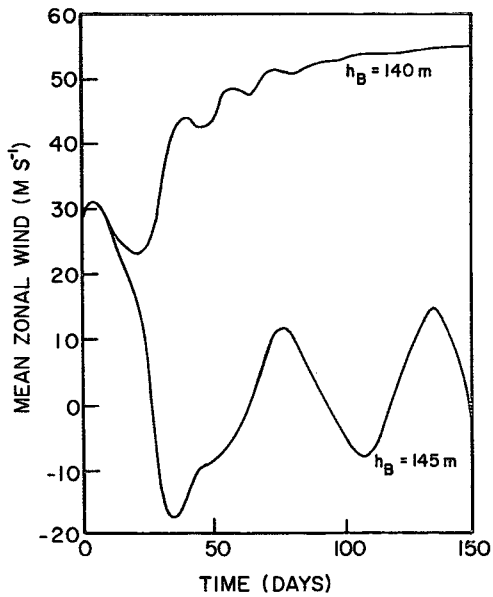

FIG. 2. Time evolutions of the mean zonal wind at 25 km and midchannel for the steady regime ($h_B = 140$ m)and the vacillating regime ($h_B = 145$ m) for zonal wavenumber 2 forcing.

In Fig. 3 the amplitudes and phases of the wave geopotential perturbation are shown for the steady state $h_B = 140$ m case and for the time-averaged component in the $h_B = 145$ m case. In the former case the wave is completely reflected by the upper level westerlies to form a standing wave and there is no upward energy flux or poleward heat flux. In the latter case the time-mean component has substantial

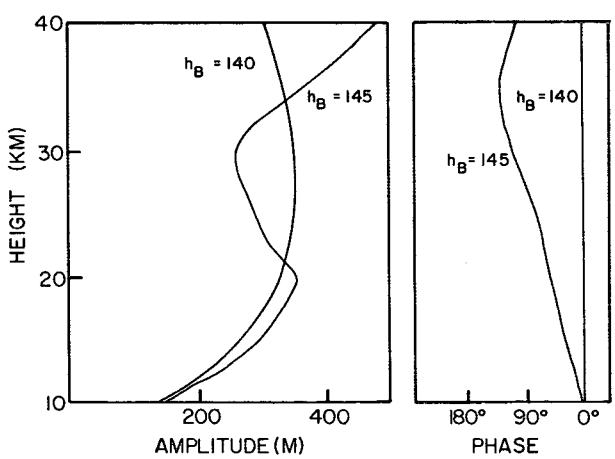

FIG. 3. Vertical profiles of the wave geopotential height perturbation amplitudes and phases averaged in time for day 180 to day 240 for the steady and vacillating regimes with zonal wavenumber 2 forcing.

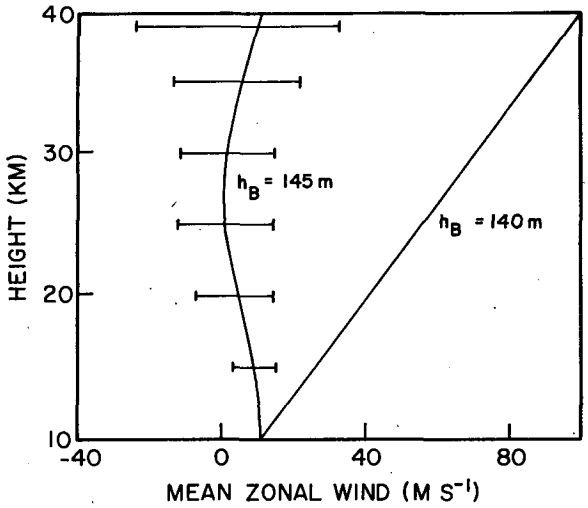

FIG. 4. Vertical profiles of the mean zonal flow averaged in time from day 180 to day 240 for the steady and vacillating regimes with zonal wavenumber 2 forcing. The crossbars indicated range of variation of the mean zonal wind at various levels for the vacillating case. The profile for the steady case is essentially identical to the radiative equilibrium profile.

westward tilt with height which implies a mean upward energy flux and poleward heat flux.

Because the time-mean adiabatic cooling vanishes in this model [see Eqs. (2) and (5)], the time-mean poleward heat flux must be balanced by differential radiative heating. Thus, in the steady wave case (where the poleward heat flux is negligible) the temperature approaches radiative equilibrium and, as shown in Fig. 4, the zonal wind profile is virtually identical to the profile for a radiative equilibrium atmosphere. In the vacillating case, however, the mean temperature departs strongly from radiative balance and the resulting zonal wind profile has very small vertical shear throughout the stratosphere. With the aid of (4) we find that in this example the time-mean differential radiative heating rate at 25 km is $\sim$1 K day^{-1} [in good agreement with Leovy (1964)], and that this heating is balanced by a mean poleward heat flux of amplitude $\sim$25 m s^{-1} K at midchannel.

In order to further substantiate the existence of two distinct flow regimes we have run a number of cases for wavenumber 2 forcing at various amplitudes of h_B. For all $h_B<140$ m the solution approaches a steady state similar to that of the $h_B=140$ m case; for all $h_B>145$ m the solution exhibits vacillations. Both the period and amplitude of the vacillations depend on the strength of the boundary forcing. Fig. 5 shows amplitudes vs time for the zonal wind oscillations at 25 km for several values of h_B. We see that as h_B increases both the period and the amplitude of the zonal wind oscillations *decrease*. The period of approximately 24 days which occurs for $h_B=300$ m is closest to the observed periods. However, although the amplitude of wavenumber 2 does occasionally reach 300 m at the 10 km level at 60°N in midwinter

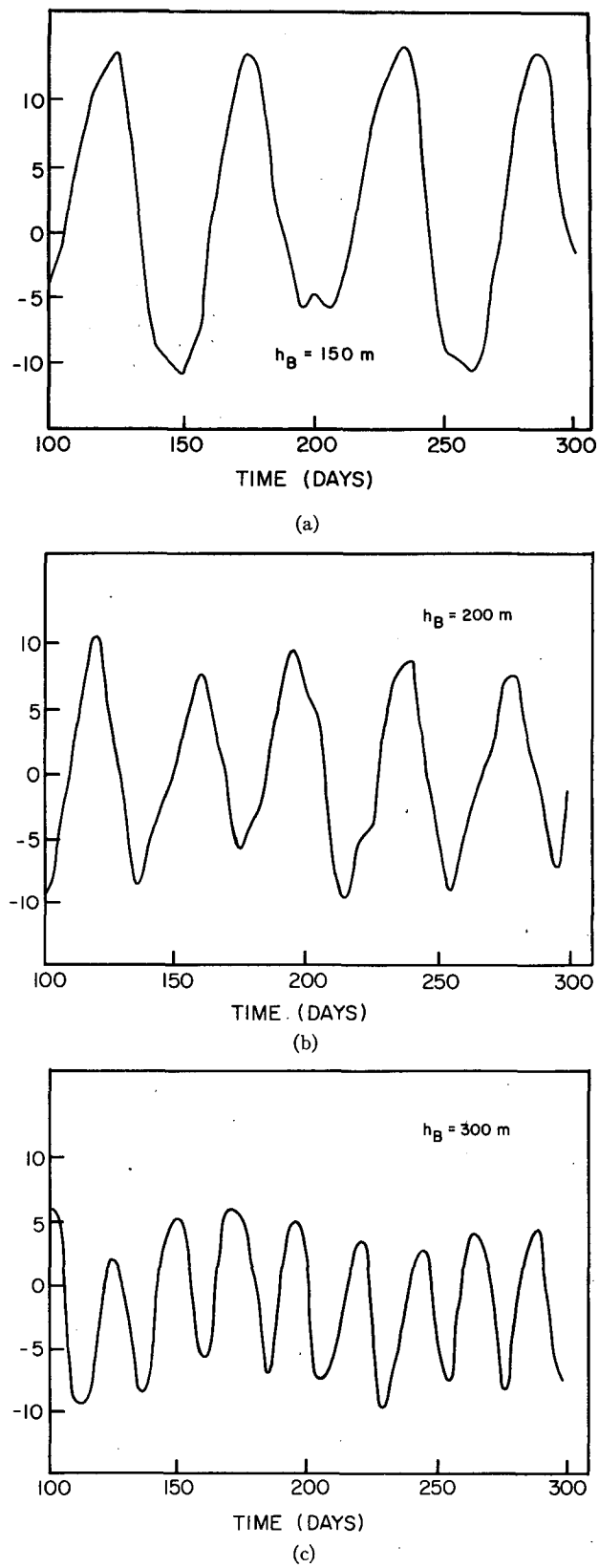

FIG. 5. Time variations of the mean zonal wind at 25 km and midchannel for zonal wavenumber 2 forcing at three different amplitudes.

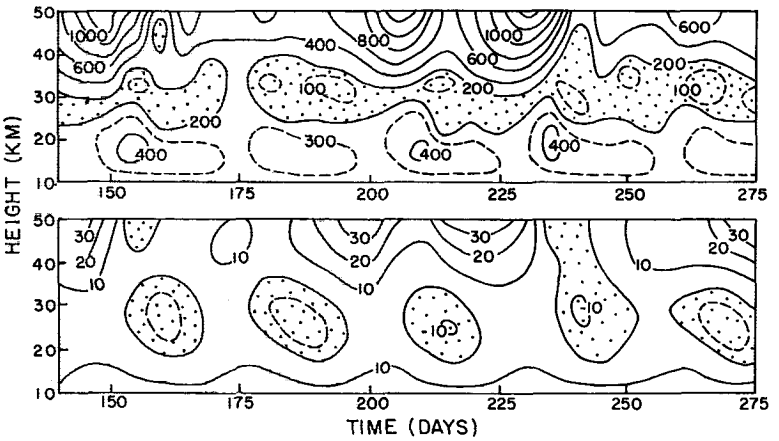

FIG. 6. Time-height sections of the geopotential height perturbation amplitude (upper) and the mean zonal wind (lower) for wavenumber 2 forcing with $h_B=250$ m. Units: height (m), zonal wind (m s^{-1}). Stippling indicates regions of negative zonal wind and geopotential amplitudes less than 200 m.

(Matsuno, 1971), the winter mean value is substantially smaller. Of course, due to the many approximations inherent in this type of mechanistic model, close agreement with observations should not be expected.

Although the periods of the zonal wind oscillations shown in Fig. 5 are quite regular there is some variation of amplitude from cycle to cycle. This variation is shown clearly in Fig. 6 where we plot time-height sections of both U_0 and $|\Psi|$ for wavenumber 2 forcing with $h_B=250$ m. Amplitudes of the oscillations in both the wave and mean wind fields vary quite strongly from cycle to cycle. This figure also illustrates the strong influence of the mean wind distribution on vertical propagation of the waves. For example, the weak westerly winds which occur throughout the stratosphere following day 222 allow the wave amplitude to build up to a maximum in the upper stratosphere by about day 230 in qualitative agreement with the planetary wave propagation theory of Charney and Drazin (1961); by day 240, however, the strong forcing of the mean flow by the waves has caused a reversal of the mean zonal flow throughout most of the stratosphere. As a consequence the waves can no longer propagate vertically, and there is rapid decay of the wave amplitude at the upper levels.

Similar irregularity in the amplitude of the wave oscillations was noted for all wavenumber 2 runs in the vacillating regime. However, such was not the case in runs with zonal wavenumber 1 forcing. In Fig. 7 time-height sections of U_0 and $|\Psi|$ are shown for a wavenumber 1 case with $h_B=300$ m. In this case, following the decay of initial transients, the wave-mean wind fields oscillate with the patterns repeating exactly every 55 days. We also found that the change from vacillation to steady state occurred at a higher value of h_B (between 150 and 200 m) than in the wavenumber 2 case. Presumably this difference in behavior is due to the fact that for a given wave amplitude the eddy potential vorticity transport is proportional to the zonal wavenumber. Again, as in the wavenumber 2 case, the trapping of the waves

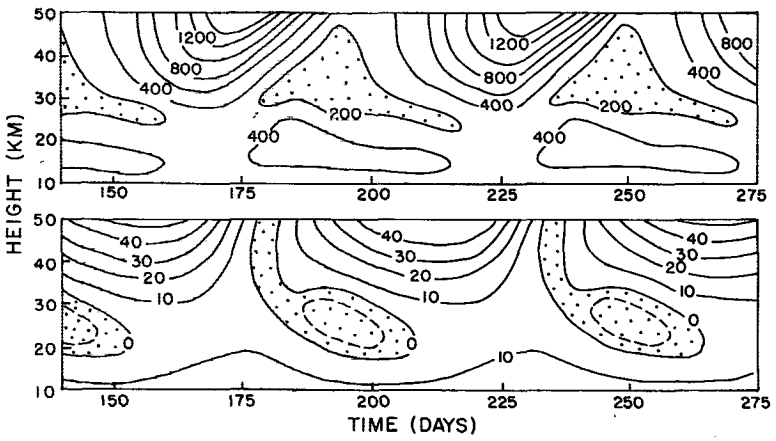

FIG. 7. As in Fig. 6 except for wavenumber 1 forcing with $h_B=300$ m.

by zonal easterlies and the enhanced propagation in weak westerlies can be clearly seen.

In conclusion we have shown that planetary waves generated by steady tropospheric forcing may interact with the stratospheric zonal wind to produce a vacillating regime in which both the waves and the mean flow oscillate in time. In a qualitative sense this vacillation cycle may be understood in terms of planetary wave propagation theory. When the mean zonal wind is westerly the stationary waves propagate upward and act to decelerate the mean flow. As soon as the mean flow becomes easterly the waves are trapped and the meridional circulation driven by the differential radiative heating restores the mean zonal westerlies. The whole process may then begin again. Thus, the present model is physically analogous to the Holton and Lindzen model for the equatorial quasi-biennial oscillation. But in the present case the time scales for the zonal wind and wave fields do not differ by an order of magnitude as is true for the quasi-biennial oscillation. Also, in the present case the zonal flow acceleration is driven primarily by wave transience rather than by wave dissipation.

In all of the model runs reported above we have held the radiative equilibrium temperature constant in time (perpetual winter). We have also carried out a few runs in which the radiative equilibrium temperature was forced to vary with an annual period by setting.

$$\bar{T}^*(y,z,t) = (20\ \mathrm{K}) \times \cos ly \sin(2\pi t/365),$$

where t is expressed in days. Not surprisingly we found that for summer heating conditions the mean zonal winds were easterly and the waves were steady and decayed rapidly in height. However, with the autumnal change to mean zonal westerlies the waves began to propagate vertically and vacillation cycles similar to those of the above models occurred until the mean zonal flow changed back to easterly in the late spring.

Finally, we note that the exclusion of higher meridional modes in this model has suppressed any barotropic energy exchanges due to horizontal momentum fluxes. In the atmosphere such barotropic processes may play an important role in stratospheric oscillations at least part of the time (Hirota and Sato, 1969). Because of this and other limitations of our model the present results should be regarded as primarily heuristic. However, we believe that this model does provide a convincing demonstration that large-scale stratospheric motions may undergo irregular vacillations even when the tropospheric forcing is steady.

Acknowledgment. This work was supported by the Atmospheric Sciences Section, National Science Foundation, under Grant ATM74-21418.

APPENDIX

The Numerical Method

In order to clarify our numerical method we shall outline the process of putting the potential vorticity equation (1) into its finite-difference analog; the $\bar{u}$ prediction equation is done in a similar way.

Combining Eq. (1) and the expressions for ψ', q', β_e and $\bar{u}$, the potential vorticity equation becomes

$$\left(\frac{\partial^2}{\partial z^2}-\frac{1}{4H^2}-K^2\right)\frac{\partial \Psi}{\partial t}+(ik\epsilon U_0+\alpha)\left(\frac{\partial^2}{\partial z^2}-\frac{1}{4H^2}\right)\Psi$$
$$+ik\left(\frac{\beta_e N^2}{f_0^2}-K^2\epsilon U_0\right)\Psi+\frac{\partial \alpha}{\partial z}\left(\frac{\partial}{\partial z}+\frac{1}{2H}\right)\Psi=0, \quad \text{(A1)}$$

where $K^2=[N^2(k^2+l^2)]/f_0^2$. We set up the finite differencing by letting $t=n\Delta t$, where $n=0, 1, 2, \cdots$, $z=(j-1)\Delta z$, where $j=1, 2, \cdots$, JM; JM corresponds to the upper boundary $z=z_T$. Furthermore, we define time average and time difference operations as

$$\left.\begin{aligned}\hat{\Psi}&=\frac{\Psi^{n+1}+\Psi^n}{2}=\Psi^{n+\frac{1}{2}}\\ \left(\frac{\partial \Psi}{\partial t}\right)^{n+\frac{1}{2}}&=\frac{\Psi^{n+1}-\Psi^n}{\Delta t}=\frac{2}{\Delta t}(\hat{\Psi}-\Psi^n)\end{aligned}\right\}.$$

Substituting these into (A1) we get

$$\left(\frac{\partial^2}{\partial z^2}-\frac{1}{4H^2}\right)\hat{\Psi}+\left[\frac{ik\Delta t}{2r}\left(\frac{\beta_e N^2}{f_0^2}-K^2\epsilon U_0\right)-\frac{K^2}{r}\right]\hat{\Psi}$$
$$+\frac{\Delta t}{2r}\frac{\partial \alpha}{\partial z}\left(\frac{\partial}{\partial z}+\frac{1}{2H}\right)\hat{\Psi}=\frac{1}{r}\left(\frac{\partial^2}{\partial z^2}-\frac{1}{4H^2}-K^2\right)\Psi^n, \quad \text{(A2)}$$

where

$$r=r(z)=\left[1+\frac{ik\Delta t\epsilon}{2}U_0(z,t)+\frac{\alpha\Delta t}{2}\right].$$

Note that this equation corresponds to (A1) at $t=(n+\frac{1}{2})\Delta t$. If we let

$$y=\frac{\Delta t}{2r}\frac{\partial \alpha}{\partial z},$$

$$Q=\frac{1}{4H^2}+\frac{1}{r}\left[K^2-\frac{ik\Delta t}{2}\left(\frac{\beta_e N^2}{f_0^2}-K^2\epsilon U_0\right)\right]-\frac{y}{2H},$$

then (A2) becomes

$$\frac{\partial^2 \hat{\Psi}}{\partial z^2}+y\frac{\partial \hat{\Psi}}{\partial z}-Q\hat{\Psi}=\frac{1}{r}\left(\frac{\partial^2}{\partial z^2}-\frac{1}{4H^2}-K^2\right)\Psi^n. \quad \text{(A3)}$$

Eq. (A3) is a two-point boundary value problem for

$\hat{\Psi}(z)$. To solve this we set

$$\left.\begin{aligned}\frac{\partial^2\hat{\Psi}}{\partial z^2}&=\frac{\hat{\Psi}_{j+1}-2\hat{\Psi}_j+\hat{\Psi}_{j+1}}{\Delta z^2}\\ \frac{\partial\hat{\Psi}}{\partial z}&=\frac{\hat{\Psi}_{j+1}-\hat{\Psi}_{j-1}}{2\Delta z}\end{aligned}\right\}.$$

Substituting these into (A3) yields

$$-M\hat{\Psi}_{j+1}-N\hat{\Psi}_{j-1}+\hat{\Psi}_j(2+B_j)=S_j, \qquad \text{(A4)}$$

where

$$\left.\begin{aligned}M&=1+\frac{y\Delta z}{2}\\ N&=1-\frac{y\Delta z}{2}\\ B_j&=(\Delta z^2)Q\\ \sigma_j&=2+\frac{\Delta z^2}{4H^2}+K^2\Delta z^2\\ S_j&=\frac{1}{r}(-\Psi_{j+1}{}^n-\Psi_{j-1}{}^n+\sigma_j\Psi_j{}^n)\end{aligned}\right\}.$$

Eq. (A4) along with the boundary conditions

$$\hat{\Psi}=0 \quad \text{at} \quad j=JM, \quad \hat{\Psi}_{j=1}=\frac{gh(t)}{f_0}$$

can be easily solved using the tridiagonal algorithm (Richtmeyer and Morton, 1967).

REFERENCES

Deland, R. J., 1973: Spectral analysis of traveling planetary scale waves: Vertical structure in middle latitudes of Northern Hemisphere. *Tellus*, **25**, 355–373.

Dickinson, R. E., 1969: Theory of planetary wave-zonal flow interaction. *J. Atmos. Sci.*, **26**, 73–81.

——, 1973: Method of parameterization for infrared cooling between altitudes of 30 and 70 kilometers. *J. Geophys. Res.*, **78**, 4451–4457.

Geisler, J. E., 1974: A numerical model of the sudden stratospheric warming mechanism. *J. Geophys. Res.*, **79**, 4989–4999.

Harwood, R. S., 1975: The temperature structure of the Southern Hemisphere stratosphere, August–October, 1971. *Quart. J. Roy. Meteor. Soc.*, **101**, 75–92.

Hirota, I., and Y. Sato, 1969: Periodic variation of the winter stratospheric circulation and intermittent vertical propagation of planetary waves. *J. Meteor. Soc. Japan*, **47**, 390–402.

Holton, J. R., 1975: *The Dynamic Meteorology of the Stratosphere and Mesosphere. Meteor. Monogr.*, No. 47, Amer. Meteor. Soc., 218 pp.

——, 1976: A semi-spectral numerical model for wave-mean flow interactions in the stratosphere: Application to the sudden stratospheric warmings. *J. Atmos. Sci.*, **33**, 1639–1649.

Leovy, C. B., 1964: Simple models of thermally driven mesospheric circulations. *J. Atmos. Sci.*, **21**, 327–341.

——, and P. J. Webster, 1976: Stratospheric long waves: Comparison of thermal structure in the Northern and Southern Hemispheres. *J. Atmos. Sci.*, **33**, 1624–1638.

Madden, R. A., 1975: Oscillations in the winter stratosphere: Part 2. The role of horizontal eddy heat transport and the interaction of transient and stationary planetary waves. *Mon. Wea. Rev.*, **103**, 717–729.

Matsuno, T., 1971: A dynamical model of the sudden stratospheric warming. *J. Atmos. Sci.*, **28**, 1479–1494.

Muench, H. S., 1965: On the dynamics of the winter stratospheric circulation. *J. Atmos. Sci.*, **22**, 349–360.

Pfeffer, R., G. Buzyna and W. W. Fowlis, 1974: Synoptic features and energetics of wave amplitude vacillation in a rotating differentially heated fluid. *J. Atmos. Sci.*, **31**, 622–645.

Quiroz, R. S., A. J. Miller and R. M. Nagatani, 1975: A comparison of observed and simulated properties of sudden stratospheric warmings. *J. Atmos. Sci.*, **32**, 1723–1736.

Richtmeyer, R. D., and K. W. Morton, 1967: *Difference Methods for Initial-Value Problems*. Wiley-Interscience, 399 pp.

Simmons, A. J., 1974: Planetary scale disturbances in the polar winter stratosphere. *Quart. J. Roy. Meteor. Soc.*, **100**, 531–540.

Trenberth, K. E., 1973: Dynamic coupling of the stratosphere with the troposphere and sudden stratospheric warmings. *Mon. Wea. Rev.*, **101**, 306–322.